



ORIGINAL ARTICLE

Open Access



Micro-FTIR spectroscopy and partial least-squares regression for rapid determination of moisture content of nanogram-scaled heat-treated wood

Hanmeng Yuan¹, Shiyao Tang², Qiuyan Luo¹, Teng Xiao¹, Wenlei Wang¹, Qiang Ma¹, Xin Guo^{1*} and Yiqiang Wu^{2*}

Abstract

Moisture sorption has a significant impact on the performance of heat-treated wood. In order to better characterize moisture sorption of heat-treated wood, a method for rapid determination of moisture content (MC) of nanogram-scaled heat-treated wood is proposed in this work. During moisture adsorption process, micro-Fourier transform infrared (FTIR) spectra of heat-treated wood were recorded. Spectral analysis was applied to these measured spectra, and then moisture adsorption sites and spectral ranges affected by moisture sorption were identified. Meanwhile, moisture contents (MCs) of heat-treated wood at various relative humidity (RH) levels were measured by using dynamic vapor sorption (DVS) setup. Based on these spectral ranges and MCs, a quantitative forecasting model was established using partial least-square regression (PLSR). Furthermore, the developed forecasting model was applied to acquire moisture sorption isotherm of heat-treated wood, in which a very positive correlation between predicted and measured MCs was observed. It was confirmed that this method was effective for rapid detection of MC of nanogram-scaled heat-treated wood which had unique advantages of rapid analysis (second level) and less sample consumption (nanogram level).

Keywords: Moisture sorption, Micro-FTIR spectroscopy, Partial least-squares regression

Introduction

Wood is a green and renewable building material, and it has been widely used in construction industry, furniture production and pulping and papermaking industry [1–3]. Heat treatment is considered to be an effective technique for wood physical modification, while moisture sorption has a significant impact on the performance of heat-treated wood [4–7]. Hence, a deeper research on moisture sorption of heat-treated wood is extremely important.

Moisture sorption, an important property of heat-treated wood, has been studied from various aspects [8–10]. Moisture content (MC) is one of the key aspects, which is mainly measured by gravimetric methods, especially dynamic vapor sorption (DVS). For example, Metsä-Kortelainen et al. [11] confirmed that heat-treated Scots pine (*Pinus sylvestris*) and Norway spruce (*Picea abies*) have lower MCs than those untreated samples whose dimensions were $22 \times 65 \times 150 \text{ mm}^3$. Besides, Hill et al. [12] employed the DVS apparatus to acquire MCs of heat-treated Scots pine (*Pinus sylvestris* L.) in the relative humidity (RH) range from 0 to 95%. Further, using DVS apparatus, the sorption isotherms of other heat-treated wood including acacia (*Acacia mangium*) [13], sesendok (*Endospermum malaccense*) [14], scots pine (*Pinus sylvestris* L.) [15–17] and *Eucalyptus pellita* [18] were

*Correspondence: guocumt@163.com; wuyq0506@126.com

¹ College of Science, Central South University of Forestry and Technology, Changsha 410004, China

² College of Material Science and Engineering, Central South University of Forestry and Technology, Changsha 410004, China

determined. Although the results are promising, DVS technique is blocked in certain problems, such as sample consumption (milligram level) and experiment time (minute level).

Many spectroscopic methods such as near-infrared spectroscopy [19, 20], Fourier transform infrared spectroscopy (FTIR) [21–23] and Raman spectroscopy [24] have been employed to study moisture sorption of heat-treated wood at molecular level. For example, Esteves et al. [25] demonstrated that the near-infrared spectroscopy has enough ability to predict MC of heat-treated pine (*Pinus pinaster*) and eucalypt (*Eucalyptus globulus*). Boonstra et al. [26] took advantage of FTIR spectroscopy to study the moisture sorption, and showed that the decrease in MC of heat-treated wood was attributed to the cross-linking of lignin and the reducing of OH group. Guo et al. [24] examined moisture sorption using Raman spectroscopy. Among these spectroscopic methods, FTIR spectroscopy has been widely applied, for it has many merits, for example: high spectral quality [27, 28], fast data collection speed [29–32], higher signal-to-noise ratio [33, 34], high sensitivity for the detection of moisture [35]. Moreover, micro-FTIR spectroscopy is a superior analytical technique for investigating micron-sized sample [36]. Through the use of a light microscope, an infrared spectrophotometer, a mercury cadmium telluride detector, and an extensive on-line software library of organic chemical spectra, this new technique is capable of identifying micron-scaled sample.

Considering that micro-FTIR spectroscopy has the ability to study micron-sized sample [37, 38], in this study, we developed a method for rapid detection of MC of nanogram-scaled heat-treated wood. First, we collected micro-FTIR spectra of nanogram-scaled heat-treated wood during moisture adsorption process. Second, these collected spectra were used to determine

moisture sorption sites and spectral ranges correlated with moisture sorption. Third, on account of these determined spectral ranges and measured MCs, the micro-FTIR forecasting model was generated. Finally, the developed forecasting model was applied to acquire moisture sorption isotherm of nanogram-scaled heat-treated wood.

Materials and methods

Sample preparation

Wood specimens (dimensions $100 \times 30 \times 10$ mm in length, width, and thickness) were collected from straight stem of *Ginkgo biloba* L. (Ginkgoaceae). Then heat treatment was used for these wood specimens in electric vacuum drying oven under controlled condition of 180 ± 1 °C. This heat treatment lasted 4 h. From these heat-treated wood specimens, transverse sections were prepared without embedding and any chemical treatment. These sections, $5 \text{ mm} \times 5 \text{ mm} \times 10 \text{ }\mu\text{m}$, were cut using a manual rotary microtome (Leica RM2135). Prior to the spectral measurement, the transverse section of heat-treated wood specimen was dried at 102 ± 3 °C in the oven for 2 h.

Experimental setup for measurement of micro-FTIR spectroscopy

Figure 1a shows an experimental setup for measurement of micro-FTIR spectroscopy. The main section of the experimental setup was a spectrometer (Nicolet IN 10). This spectrometer included one microscope which provided a new function for selecting observation area. During the spectral measurement, one observation area ($30 \text{ }\mu\text{m}$ by $30 \text{ }\mu\text{m}$) was randomly selected in the transverse section of heat-treated wood specimen, in which small quantities ($\sim 1 \text{ ng}$) of heat-treated wood was present. The micro-FTIR spectroscopy in the wavenumber

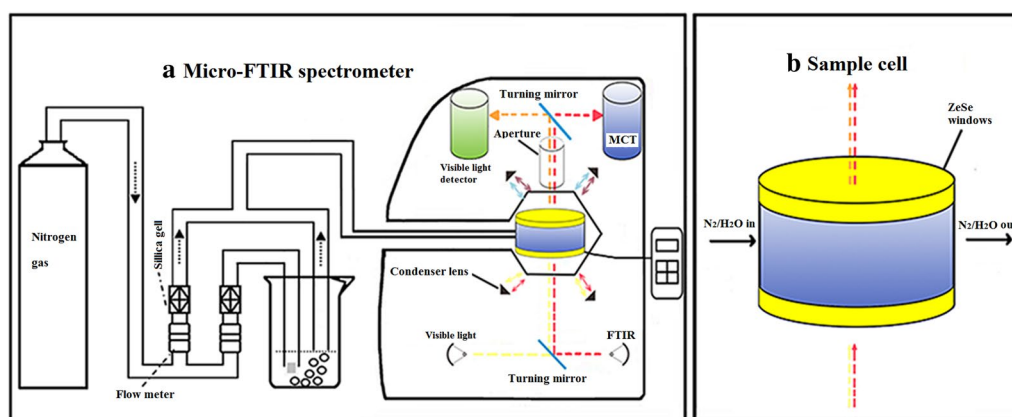


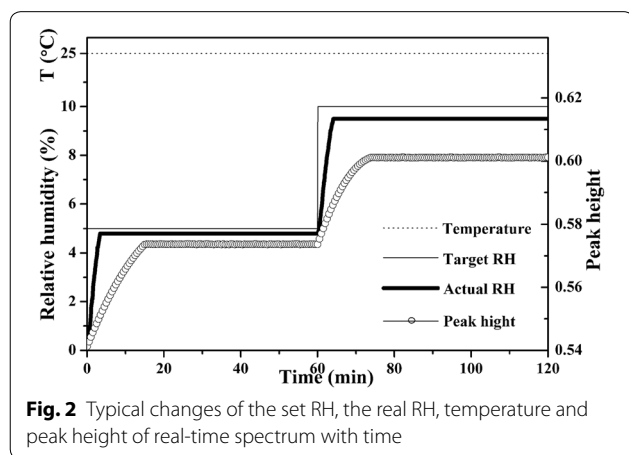
Fig. 1 Experimental setup for measurement of micro-FTIR spectroscopy

range from 720 to 4000 cm^{-1} was recorded with 4 cm^{-1} resolution; 32 scans were collected. Meanwhile, the spectral data were recorded at a constant temperature of 25 °C. Figure 1b shows the sample cell. One prepared transverse section was placed on the base of sample cell which was made of ZnSe plate. Then this sample cell was mounted on the stage of the spectrometer. Meanwhile, through this sample cell, nitrogen gas with specific RH was circulated.

Before the spectral measurement, a kinetic spectroscopy test was conducted to calculate the balance time. Figure 2 shows typical changes of the set RH, the real RH, temperature and peak height of real-time spectrum with time. When the set RH was changed to a new value (such as 5 and 10%), the latency of 3–4 min appeared. During the latency period, the real RH was more and more close to the set RH, and then arrived at stabilization. Meanwhile, 15 min later the real-time spectrum nearly did not change (peak height of the main peak at 3352 cm^{-1} associated with moisture sorption was advocated to detect spectral change). Based on these results, 60 min were set as the balance time.

Determination of MC using DVS apparatus

Moisture content was measured using DVS apparatus (DVS AdvantagePlus). First, a heat-treated wood sample was put on the sample tray which was hung on the microbalance which was situated in a thermostatically controlled cabinet. The apparatus recorded sample mass at the set RH (adsorption): 0, 5, 10, 15, 20, 25, 30, 35, 40, 45, 50, 55, 60, 65, 70, 75, 80, 85, 90 and 95%, at a temperature of 25 °C and in the reverse sequence for the desorption isotherm. Meanwhile, every set RH was maintained for enough time until the sample mass of the heat-treated wood specimen altered less than 0.002% per minute during 10 min.



Moisture content was calculated using the following formula:

$$MC = \frac{m - m_d}{m_d} \times 100, \quad (1)$$

where m_d was dry sample mass and m is real-time sample mass.

Figure 3 shows typical changes of MC and RH with time. When the set RH was changed to the next value (for example, 5 and 10%), a time delay of 4–10 min appeared. During the latency period, the real RH got close to the set RH, and then arrived at stabilization afterward. Therefore, MC would increase to a steady value at the set RH which was recorded as reference value. It should be noticed that three replicates were exposed and each MC collected as reference value was mean of three replicates.

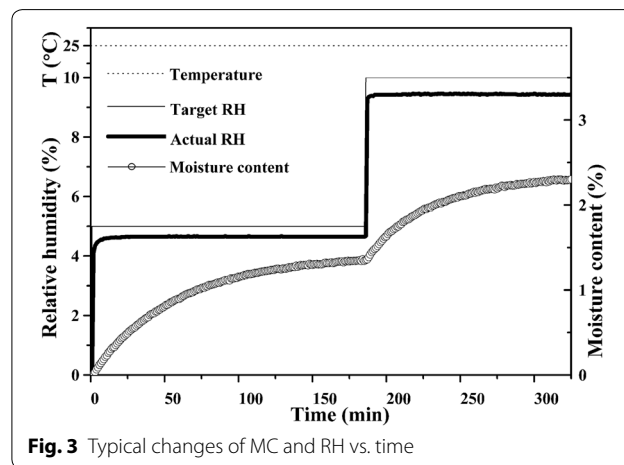
Spectral data processing

Acquiring difference spectrum

To further analyze the moisture sorption of heat-treated wood qualitatively and quantitatively, a difference spectrum technique was introduced.

Establishment of the forecasting model based on micro-FTIR spectra

A micro-FTIR forecasting model was generated using TQ Analyst™ qualitative and quantitative analysis software, one of the OMNIC software suites. In description table, quantitative analysis was set to “partial least squares”. In pathlength table, pathlength type was set to “constant”. In components table, component was set to “moisture content” whose maximum and minimum values were both entered, and these two values were acquired using DVS apparatus. In standards table, sample spectra collected at 35 different relative humidities were introduced. Four-fifths of sample spectra measured at 28 different relative



humidities with six replicates (i.e., 168 spectra) were assigned to the calibration set, and the remaining sample spectra acquired at seven different relative humidities with six replicates (i.e., 42 spectra) were allocated to the validation set. In spectra table, no smoothing and multipoint baseline correction were programmed. In regions table, spectral range was adjusted according to the qualitative description of heat-treated wood moisture sorption. When these parameters were enabled, the TQ Analyst™ qualitative and quantitative analysis software program was run, and one forecasting model was established. Model performance was estimated using the correlation of determination (R^2), root-mean-square error of cross-validation (RMSECV) and root-mean-square error of prediction (RMSEP).

Results and discussion

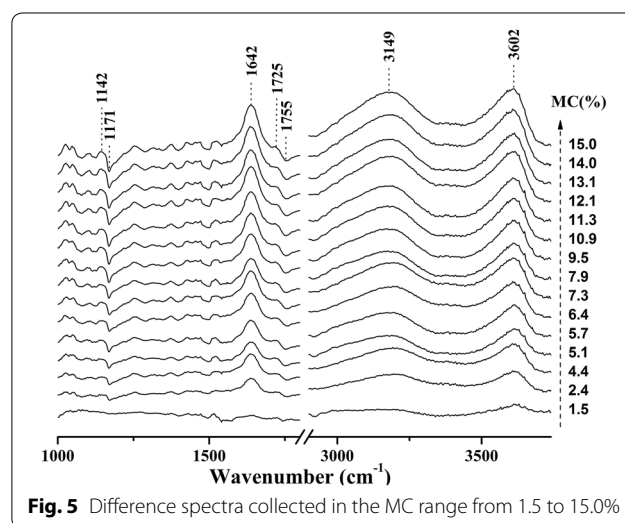
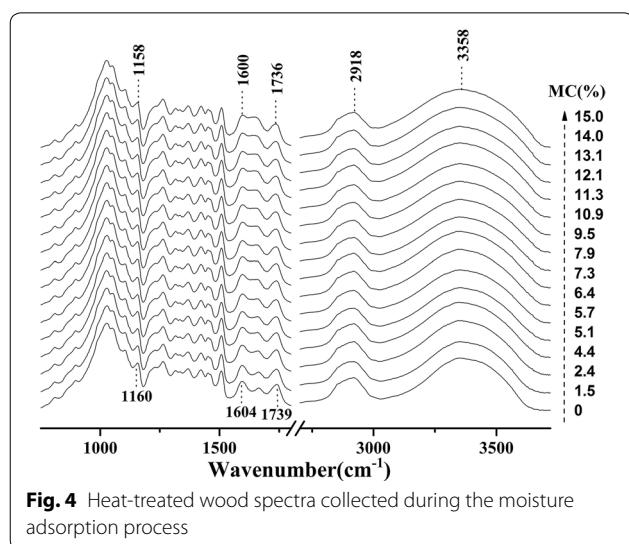
Qualitatively analyzing moisture sorption in heat-treated wood

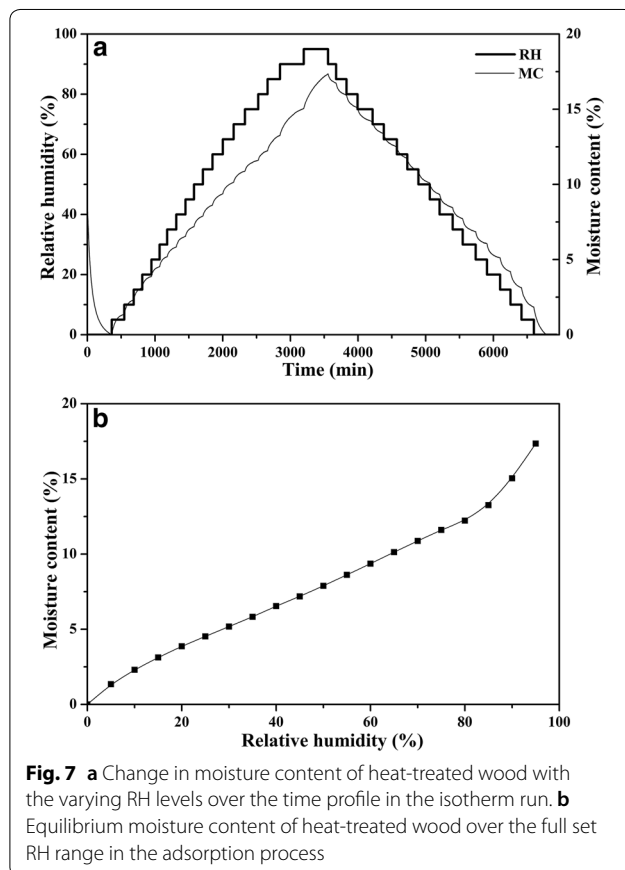
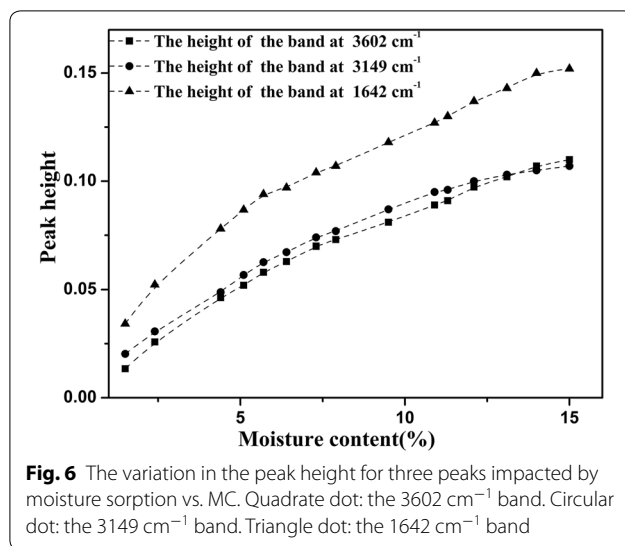
Figure 4 shows heat-treated wood spectra collected at the moisture adsorption process. The development of micro-FTIR spectra could be seen over a range of MC from 0 to 15.0% in this figure. At the MC of 15.0%, the main band at 3358 cm^{-1} assigned to O–H stretching vibration increased, showing the OH group was moisture adsorption sites of heat-treated wood. The band at 1736 cm^{-1} was assigned to C=O stretching vibration of carboxylic acid, the 1600 cm^{-1} band belonged to the aromatic skeletal vibration plus the C=O stretching vibration, and the band at 1158 cm^{-1} was attributed to the glucosidic C–O–C vibration. For comparison, heat-treated wood spectrum measured at 0% MC was also displayed, in which these three bands appeared at 1739, 1604, and 1160 cm^{-1} . When RH increased, the band

positions of these three bands exhibited continuous red shifts. These peak shifts indicated the carbonyl and C–O groups were moisture adsorption sites of heat-treated wood. What's more, it was confirmed that two micro-FTIR spectral ranges correlated with moisture sorption were $3700\text{--}3100$ and $1780\text{--}1700\text{ cm}^{-1}$.

Figure 5 presents difference spectra at various MC levels during the moisture adsorption process. The broad envelope range of $3700\text{--}2800\text{ cm}^{-1}$ containing many component bands was observed to rise which resulted from moisture sorption. Further, the first spectral range correlated with moisture sorption was precisely identified as from 3700 to 2800 cm^{-1} . Meanwhile, the 1755 cm^{-1} band belonged to free carbonyl group decreased, while the 1725 cm^{-1} band was assigned to hydrogen bonded carbonyl group had reverse trend. Meanwhile, the band around 1642 cm^{-1} was assigned to H–O–H bending vibration. Therefore, second spectral range was precisely identified as from 1770 to 1580 cm^{-1} . Moreover, with an increase of RH, the 1171 cm^{-1} band was shown to decrease, while the 1142 cm^{-1} band was found to rise. The same reflections were happened in two bands located at 1171 and 1142 cm^{-1} . This further suggested the third spectral range correlated with moisture sorption could be precisely confirmed as from 1180 to 1140 cm^{-1} .

Further, the variation in the peak height for three peaks impacted by water sorption vs. MC is shown in Fig. 6. Clearly the variation for three peaks was diverse, suggesting that water molecule was absorbed by all these sorption sites. However, none of these three peaks could predict moisture sorption isotherm. Therefore, a method for determination of MC of heat-treated wood is needed urgently.





Quantitative detection of MC of heat-treated wood

As shown previously, DVS has offered vast amounts of moisture sorption isotherms [39–41]. Hence, this technique was introduced to collect MCs as measured values. Figure 7 shows the experimental sorption isotherm. This

isotherm curve presented a typical sigmoidal shape commonly observed for other lignocellulosic materials [42].

In order to establish a method for rapid determination of MC, the forecasting model based on micro-FTIR spectroscopy ought to be determined firstly. As mentioned earlier, spectral range was an important parameter for the forecasting model. Three spectral ranges of 3700–2800, 1770–1580, and 1180–1140 cm^{-1} correlated with moisture sorption were proposed as Case A. Further, the widened and narrowed spectral ranges were introduced separately as Case B and C (Case B: 3700–2800, 2800–2700, 1770–1580, and 1180–1140 cm^{-1} ; Case C: 3700–3000, 1770–1580, and 1180–1140 cm^{-1}). In all three cases, the micro-FTIR forecasting model was generated and corresponding parameters such as RESECV, RESEP, and R^2 could be acquired in TQ Analyst™ software (as shown in Table 1). The established forecasting model in Case A had highest forecast accuracy, for it possessed highest values of R^2 as well as the lowest values of RMSEP and RMSECV. What's more, this model made use of the whole spectral ranges correlated with moisture sorption, and the change of spectral range (increase and decrease) could decrease the accuracy of the established forecasting model in Case B and C.

Based on the established forecasting model, MCs of heat-treated wood were predicted. Moreover, measured values using DVS setup are displayed in Fig. 8. During the moisture adsorption process, the predicted MCs were much closed to the measured values (relative error was lower than 3%). Results indicated that this method for rapid detection of MC in nanogram-scaled heat-treated wood using micro-FTIR spectroscopy and partial least-squares regression was effective and efficient. Compared to the traditional DVS, it has unique advantages of rapid analysis (second level) and less sample consumption (nanogram level).

Conclusion

One method for rapid determination of moisture content of nanogram-scaled heat-treated wood was proposed here. Micro-FTIR spectra were measured during the moisture adsorption process. An analysis of these spectra confirmed that hydroxyl and carbonyl groups were moisture sorption sites of heat-treated wood. Moreover, three spectral ranges, such as 3700–2800, 1770–1580, and 1180–1140 cm^{-1} were identified that related to moisture sorption. Based on these three spectral ranges and referential values, a quantitative forecasting model was built using PLSR. Further, the developed forecasting model was applied to acquire moisture sorption isotherm of heat-treated wood, in which a very positive correlation between the forecasts and recorded values. It was confirmed that this method

Table 1 PLSR quality parameters for cross- and test set-validation for the proposed three cases

	First case	Second case	Third case
Spectral region (cm ⁻¹)	3700–2800/1770–1580/1180–1140	3700–2800/2800–2700/1770–1580/1180–1140	3700–3000/1770–1580/1180–1140
Cross-validation			
RMSECV (%)	50.5	73.6	54.3
Number of PLS components	6	6	6
R ²	0.9945	0.9898	0.9937
External validation			
RMSEP (%)	19.3	28.9	25.2
Number of PLS components	6	6	6
R ²	0.9988	0.9982	0.9976

RMSECV: root-mean-square error of cross-validation; RMSEP: root-mean-square error of prediction; R²: coefficient of determination

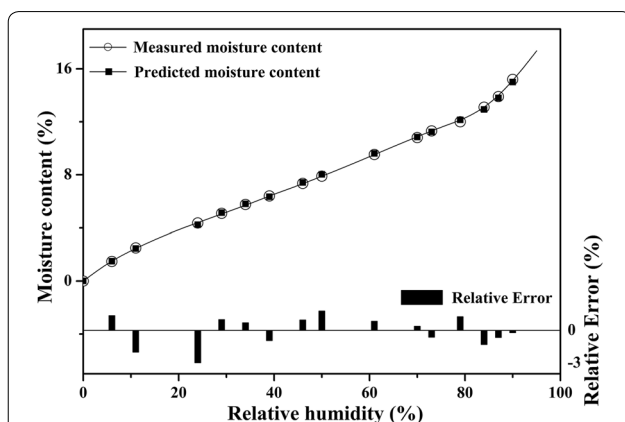


Fig. 8 Moisture sorption isotherm estimated by micro-FTIR forecasting model and that measured by DVS approach. Solid quadrate spot: MCs predicted using micro-FTIR forecasting model. Hollow circular spot: MCs measured using DVS setup

for rapid detection of moisture content in nanogram-scaled heat-treated wood was effective which had unique advantages of rapid analysis (second level) and less sample consumption (nanogram level).

Abbreviations

FTIR: Fourier transform infrared; MCs: moisture contents; RH: relative humidity; DVS: dynamic vapor sorption; PLSR: partial least-square regression; MC: moisture content; RMSECV: root-mean-square error of cross-validation; RMSEP: root-mean-square error of prediction.

Acknowledgements

The authors are grateful for the financial support from National Natural Science Foundation of China (Grant Numbers 31890771, 31670563 and 31500475), Special projects of scientific and technological innovation in Hunan forestry (Grant No. XLK201982), Natural Science Foundation of Hunan Province, China (Grant Number 2019JJ50981), Research Foundation of Education Bureau of Hunan Province, China (Grant Number 18A166), and Scientific Innovation Fund for Post-graduates of Central South University of Forestry and Technology (Grant Number CX20192073).

Authors' contributions

All the authors have contributed to the manuscript and take all responsibilities for the entire content of the manuscript. All authors read and approved the final manuscript.

Funding

This study was supported by National Natural Science Foundation of China (Grant Numbers 31890771, 31670563 and 31500475), Special projects of scientific and technological innovation in Hunan forestry (Grant No. XLK201982), Natural Science Foundation of Hunan Province, China (Grant Number 2019JJ50981), Research Foundation of Education Bureau of Hunan Province, China (Grant Number 18A166), and Scientific Innovation Fund for Post-graduates of Central South University of Forestry and Technology (Grant Number CX20192073).

Availability of data and materials

The datasets used or analyzed during the current study are available from the corresponding author on reasonable request.

Competing interests

The authors declare that they have no competing interests.

Received: 3 August 2019 Accepted: 8 January 2020

Published online: 16 January 2020

References

- Wälinder MEP, Gardner DJ (1999) Factors influencing contact angle measurements on wood particles by column wicking. *J Adhes Sci Technol* 13:1363–1374
- Obataya E, Norimoto M, Gril J (1998) The effects of adsorbed water on dynamic mechanical properties of wood. *Polymer* 39:3059–3064
- Maeda H, Fukada E (1987) Effect of bound water on piezoelectric, dielectric, and elastic properties of wood. *J Appl Polym Sci* 33:1187–1198
- Rekola J, Aho AJ, Gunn J, Matinlinna J, Hirvonen J, Viitaniemi P, Vallittu PK (2009) The effect of heat treatment of wood on osteoconductivity. *Acta Biomater* 5:1596–1604
- Kartal SN, Hwang WJ, Imamura Y (2007) Water absorption of boron-treated and heat-modified wood. *J Wood Sci* 53:454–457
- Salmen L, Possler H, Stevanic JS, Stanzltschegg SE (2008) Analysis of thermally treated wood samples using dynamic FT-IR-spectroscopy. *Holzforschung* 62:676–678
- Pelit H, Budakçı M, Sönmez A, Burdurlu E (2015) Surface roughness and brightness of scots pine (*Pinus sylvestris*) applied with water-based varnish after densification and heat treatment. *J Wood Sci* 61:586–594
- Temiz A, Terziev N, Jacobsen B, Eikenes M (2010) Weathering, water absorption, and durability of silicon, acetylated, and heat-treated wood. *J Appl Polym Sci* 102:4506–4513

9. Huang X, Kocaefe D, Kocaefe Y, Boluk Y, Pichette A (2012) Changes in wettability of heat-treated wood due to artificial weathering. *Wood Sci Technol* 46:1215–1237
10. Wang Y, Iida I, Minato K (2007) Mechanical properties of wood in an unstable state due to temperature changes, and analysis of the relevant mechanism IV: effect of chemical components on destabilization of wood. *J Wood Sci* 53:381–387
11. Metsä-Kortelainen S, Antikainen T, Viitaniemi P (2006) The water absorption of sapwood and heartwood of Scots pine and Norway spruce heat-treated at 170 °C, 190 °C, 210 °C and 230 °C. *Eur J Wood Wood Prod* 64:192–197
12. Hill CAS, Ramsay J, Keating B, Laine K, Rautkari L, Hughes M, Constant B (2012) The water vapour sorption properties of thermally modified and densified wood. *J Mater Sci* 47:3191–3197
13. Willems W (2014) The water vapor sorption mechanism and its hysteresis in wood: the water/void mixture postulate. *Wood Sci Technol* 48:499–518
14. Jalaludin Z, Hill CAS, YanJun X, Samsi HW, Husain H, Awang K, Curling SF (2010) Analysis of the water vapour sorption isotherms of thermally modified acacia and sesendok. *Wood Mater Sci Eng* 5:194–203
15. Hosseinpourpia R, Adamopoulos S, Holstein N, Mai C (2017) Dynamic vapour sorption and water-related properties of thermally modified Scots pine (*Pinus sylvestris* L.) wood pre-treated with proton acid. *Polym Degrad Stabil* 138:161–168
16. Kymäläinen M, Mlouka SB, Belt T, Merk V, Liljeström V, Hänninen T, Uimonen T, Kostianen M, Rautkari L (2018) Chemical, water vapour sorption and ultrastructural analysis of Scots pine wood thermally modified in high-pressure reactor under saturated steam. *J Mater Sci* 53:3027–3037
17. Hosseinpourpia R, Adamopoulos S, Mai C (2017) Effects of acid pre-treatments on the swelling and vapor sorption of thermally modified scots pine (*Pinus sylvestris* L.) wood. *BioResources* 13:331–345
18. Sun B, Wang Z, Liu J (2017) Changes of chemical properties and the water vapour sorption of *Eucalyptus pellita* wood thermally modified in vacuum. *J Wood Sci* 63:133–139
19. Mitsui K, Inagaki T, Tsuchikawa S (2008) Monitoring of hydroxyl groups in wood during heat treatment using NIR spectroscopy. *Biomacromolecules* 9:286–288
20. Sandak A, Sandak J, Allegretti O (2015) Quality control of vacuum thermally modified wood with near infrared spectroscopy. *Vacuum* 114:44–48
21. Akgül M, Gümüşkaya E, Korkut S (2007) Crystalline structure of heat-treated Scots pine [*Pinus sylvestris* L.] and Uludağ fir [*Abies nordmanniana* (Stev.) subsp. *Bornmuelleriana* (Mattf.)] wood. *Wood Sci Technol* 41:281–289
22. Özgenç Ö, Durmaz S, Boyacı IH, Eksi-Kocak H (2017) Determination of chemical changes in heat-treated wood using ATR-FTIR and FT Raman spectrometry. *Spectrochim Acta A* 171:395–400
23. Kotilainen RA, Toivanen TJ, Alén RJ (2000) FTIR monitoring of chemical changes in softwood during heating. *J Wood Chem Technol* 20:307–320
24. Guo X, Wu Y, Yan N (2016) Characterizing spatial distribution of the adsorbed water in wood cell wall of *Ginkgo biloba* L. by u-FTIR and confocal Raman spectroscopy. *Holzforchung* 71:415–423
25. Esteves B, Pereira H (2008) Quality assessment of heat-treated wood by NIR spectroscopy. *Holz als Roh- und Werkstoff* 66:323–332
26. Boonstra MJ, Tjeerdsmas B (2006) Chemical analysis of heat treated softwoods. *Holz als Roh- und Werkstoff* 64:204–211
27. Gerwert K, Hess B, Michel H, Buchanan S (1988) FTIR studies on crystals of photosynthetic reaction centers. *FEBS Lett* 232:303–307
28. Zhang J, Zhang X, Zhang F, Yu S (2017) Solid-film sampling method for the determination of protein secondary structure by Fourier transform infrared spectroscopy. *Anal Bioanal Chem* 409:4459–4465
29. Jangir DK, Charak S, Mehrotra R, Kundu S (2011) FTIR and circular dichroism spectroscopic study of interaction of 5-fluorouracil with DNA. *J Photochem Photobiol B* 105:143–148
30. Bunaciu AA, Aboul-Enein HY, Fleschin S (2012) FTIR spectrophotometric methods used for antioxidant activity assay in medicinal plants. *Appl Spectrosc Rev* 47:245–255
31. Amir RM, Anjum FM, Khan MI, Khan MR, Pasha I (2013) Application of Fourier transform infrared (FTIR) spectroscopy for the identification of wheat varieties. *J Food Sci Technol* 50:1018–1023
32. Ahmad I, Ullah J, Ishaq M, Khan H, Gul K, Siddiqui S, Ahmad W (2015) Monitoring of oxidation behavior in mineral base oil additized with biomass derived antioxidants using FT-IR spectroscopy. *RSC Adv* 5:101089–101100
33. González-Gaitano G, Isasi JR (2001) Analysis of the rotational structure of CO₂ by FTIR spectroscopy. *Chem Educ* 6:362–364
34. Heidi N, Nils Kristian A, Young JF, Bertram HC, Pedersen ME, Stine G, Gjermund V, Achim K (2011) Monitoring cellular responses upon fatty acid exposure by Fourier transform infrared spectroscopy and Raman spectroscopy. *Analyst* 136:1649–1658
35. Céline A, Goncalves O, Jacquemin F, Fréour S (2014) Qualitative and quantitative assessment of water sorption in natural fibres using ATR-FTIR spectroscopy. *Carbohydr Polym* 101:163–170
36. Yong L, Zhiwei Y, Yury D, Gassman PL, Hai W, Alexander L (2008) Hygroscopic behavior of substrate-deposited particles studied by micro-FT-IR spectroscopy and complementary methods of particle analysis. *Anal Chem* 80:633
37. Guo X, Liu L, Wu J, Fan J, Wu Y (2018) Qualitatively and quantitatively characterizing water adsorption of a cellulose nanofiber film using micro-FTIR spectroscopy. *RSC Adv* 8:4214–4220
38. He X, Leng C, Pang S, Zhang Y (2017) Kinetics study of heterogeneous reactions of ozone with unsaturated fatty acid single droplets using micro-FTIR spectroscopy. *RSC Adv* 7:3204–3213
39. Argyropoulos D, Alex R, Kohler R, Muller J (2012) Moisture sorption isotherms and isosteric heat of sorption of leaves and stems of lemon balm (*Melissa officinalis* L.) established by dynamic vapor sorption. *LWT Food Sci Technol* 47:324–331
40. Garbalinska H, Bochenek M, Malorny W, Von Werder J (2017) Comparative analysis of the dynamic vapor sorption (DVS) technique and the traditional method for sorption isotherms determination—exemplified at autoclaved aerated concrete samples of four density classes. *Cement Concr Res* 91:97–105
41. Fang L, Xiong X, Wang X, Hong C, Mo X (2016) Effects of surface modification methods on mechanical and interfacial properties of high-density polyethylene-bonded wood veneer composites. *J Wood Sci* 63:65–73
42. Avramidis S (1989) Evaluation of “three-variable” models for the prediction of equilibrium moisture content in wood. *Wood Sci Technol* 23:251–257

Publisher's Note

Springer Nature remains neutral with regard to jurisdictional claims in published maps and institutional affiliations.